A Comparative Analysis on Single and Two Phase Casson Fluid under Aligned Magnetic Field Effect and Newtonian Heating

Tijjani Lawal Hassan[1], Abdul Rahman Mohd Kasim[2,3,*], Mohd Haziezan Hassan[2]

[1]   School of General Studies, Kano State Polytechnic, PMB 3401, BUK Road, Gwale, Kano, Nigeria
[2]   Centre for Mathematical Sciences, Universiti Malaysia Pahang Al-Sultan Abdullah, Lebuh Persiaran Tun Khalil Yaakob, Gambang, 26300, Malaysia
[3]   Center for Research in Advanced Fluid and Process, Universiti Malaysia Pahang Al-Sultan Abdullah, Lebuh Persiaran Tun Khalil Yaakob, Gambang, Kuantan 26300, Pahang, Malaysia

ARTICLE INFO	ABSTRACT
	This research investigates the impact of aligned magnetic fields and Newtonian heating on single and two-phase Casson fluid (a mixture of Casson fluid and dust particles), addressing a notable knowledge gap in comparing the two fluid models under the same effect. The problem of this study lies in the need to understand the similarities or differences in the reaction of these fluids to external forces. To achieve this, the governing equations for both fluids were formulated using a boundary layer approximation and numerical solutions were obtained utilizing the 'bvp4c' function within MATLAB software. The analysis revealed comparable trends in flow and thermal behaviour between the two fluids, it also showed that the magnetic field exerted a more pronounced influence on flow properties compared to forces such as buoyancy and inertia. Conversely, Newtonian heating conditions had a more significant impact on thermal properties compared to the magnetic field. Additionally, the single-phase Casson fluid showed higher velocity and temperature profiles than the two-phase Casson fluid phases. These findings suggest that the presence of dust particles reduces the velocity and temperature magnitudes of the Casson fluid.

1. Introduction

In industrial processes, fluids are often subjected to external forces that significantly affect their flow behavior and thermal characteristics. Two key external factors considered in this study are aligned magnetic fields and Newtonian heating (NH) boundary conditions. Aligned magnetic field are simply magnetic fields applied at a non-perpendicular and non-parallel manner. In this study the field is applied at an acute angle. The application of an aligned magnetic field at an acute angle leads to intriguing phenomena such as the activation of Lorentz forces, the occurrence of MHD waves, and potential MHD instability, all of which have profound implications for fluid flow patterns and thermal properties of a fluid. Newtonian heating (NH), on the other hand, refers to the transfer of heat from

a solid surface to the surrounding fluid, causing the fluid to flow due to natural convection. This definition of NH was adopted from Merkin [1] who further explained that the heat is transferred in proportion to local surface temperature, i.e., the more the surface temperature, the more the heat transfer. A considerable amount research works on NH has been done based on Merkin's definition [2-6].

Non-Newtonian fluids, exhibit flow behavior that differs from traditional Newtonian fluids and possess various industrial applications such as designing efficient systems, optimizing industrial processes, and improving product quality. Among different non-Newtonian fluid models, the Casson fluid stands out due to its ability to accurately represent the flow characteristics of various viscoelastic materials. Casson fluids are shear-thinning/pseudo-plastic non-Newtonian fluids with infinite viscosity at zero shear rate and zero viscosity at infinite shear rate. They exhibit interesting behavior, acting like solids when the shear stress is lower than the yield stress and tending to flow when the shear stress is greater than the yield stress. These fluids are modeled based on the Casson equation, which accurately describes the rheological properties of fluids exhibiting yield stress behavior. Examples of Casson fluids include molten polymers, biological fluids, and suspensions.

In practical applications, fluids exist in different phases, each with distinct properties and behaviors. Multi-phase flows, such as two-phase flows, are common in various industrial processes, including oil and gas production, chemical reactions, and separation techniques. Two-phase flows can involve different combinations of phases, such as liquid-liquid, liquid-gas, solid-liquid, or gas-gas. This research focuses comparing single-phase Casson (liquid) fluid with a two-phase flow in the form of a mixture of a single-phase Casson fluid and dust particles. This mixture is referred to as dusty Casson fluids. The underlying properties of these types of phase flows is essential for predicting and enhancing processes involving multi-phase systems, as such, numerous authors investigated fluid flow problems in two-phase, and single-phase flows [7-14].

While considerable research has been conducted on the impact of magnetic fields and Newtonian heating on different fluid models, there is a significant knowledge gap regarding the comparative analysis of single-phase and dusty Casson fluid models under the combined influence of an aligned magnetic field and Newtonian heating boundary conditions. Existing studies such as Arifin *et al.,* [7] and Kasim *et al.,* [9], have primarily focused on analyzing dusty Casson fluid without directly comparing it to the single-phase Casson fluid. Consequently, the objective of this study is to perform a comprehensive comparative analysis of single-phase and dusty Casson fluid models under the influence of an aligned magnetic field and Newtonian heating boundary conditions. The study aims to examine the influence of multiple parameters on various flow characteristics and heat transfer mechanisms to enhance our understanding of these fluids under such conditions.

2. Problem Formulation

The studied flow configuration involves a two-dimensional, incompressible, steady, and laminar boundary layer flow of a non-Newtonian Casson fluid in both single-phase and two-phase flow. In the single-phase flow, only the fluid phase is present, while in the two-phase flow, a mixture of the fluid phase and dust phase is considered. The dust particles are assumed to be spherical in shape with equal radii and uniform density. The flow occurs over a vertical and linear stretching sheet and is influenced by a magnetic field of strength B_0 at an aligned acute angle α. The system also incorporates the Newtonian Heating boundary condition. Figure 1 below illustrates this configuration.
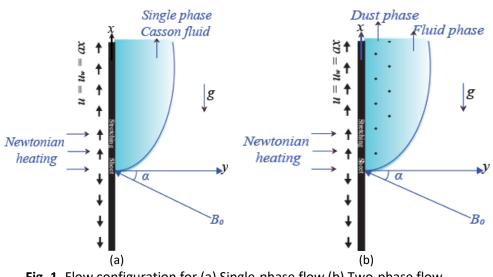
Fig. 1. Flow configuration for (a) Single-phase flow (b) Two-phase flow

Kasim *et al.,* [9] derived the governing equation for the dusty two-phase Casson fluid under the aforementioned configuration, employing boundary layer and Boussinesq approximations as follows.

Two-Phase

Fluid phase:

$$\frac{\partial u}{\partial x} + \frac{\partial v}{\partial y} = 0, \tag{1}$$

$$\rho\left(u\frac{\partial u}{\partial x} + v\frac{\partial u}{\partial y} \right) = \mu_B\left(1 + \frac{1}{\beta}\right)\left(\frac{\partial^2 u}{\partial y^2}\right) + \rho g \beta^*\left(T - T_\infty\right) + \frac{\rho_p}{\tau_v}\left(u_p - u\right) - \sigma u B_0^2 \sin^2 \alpha, \tag{2}$$

$$\rho c_p\left(u\frac{\partial T}{\partial x} + v\frac{\partial T}{\partial y} \right) = \kappa\left(\frac{\partial^2 T}{\partial y^2}\right) + \frac{\rho_p c_s}{\gamma_T}\left(T_p - T\right). \tag{3}$$

Dust phase:

$$\frac{\partial u_p}{\partial x} + \frac{\partial v_p}{\partial y} = 0, \tag{4}$$

$$\rho_p\left(u_p\frac{\partial u_p}{\partial x} + v_p\frac{\partial u_p}{\partial y} \right) = \frac{\rho_p}{\tau_v}\left(u - u_p\right), \tag{5}$$

$$\rho_p c_s\left(u_p\frac{\partial T_p}{\partial x} + v_p\frac{\partial T_p}{\partial y} \right) = \frac{\rho_p c_s}{\gamma_T}\left(T_p - T\right), \tag{6}$$

with corresponding boundary conditions

$$u = u_w(x) = ax, \ v = 0, \frac{\partial T}{\partial y} = -h_s T \ at \ y = 0,$$

$$u \to 0, u_p \to 0, v_p \to v, T \to T_\infty, T_p \to T_\infty \ as \ y \to \infty. \tag{7}$$

By definition, single phase has no dust particle, hence to obtain the governing equation with boundary condition for single phase Casson fluid under the same configuration and assumption, we set $\rho_p, u_p, v_p, T_p = 0$ in Eq. (2), Eq. (3) and Eq. (7) while leaving Eq. (1) as it is. This gives:

Single-phase

$$\frac{\partial u}{\partial x} + \frac{\partial v}{\partial y} = 0, \tag{8}$$

$$\rho \left(u \frac{\partial u}{\partial x} + v \frac{\partial u}{\partial y} \right) = \mu_B \left(1 + \frac{1}{\beta} \right) \left(\frac{\partial^2 u}{\partial y^2} \right) + \rho g \beta^* (T - T_\infty) - \sigma u B_0^2 \sin^2 \alpha, \tag{9}$$

$$\rho c_p \left(u \frac{\partial T}{\partial x} + v \frac{\partial T}{\partial y} \right) = \kappa \left(\frac{\partial^2 T}{\partial y^2} \right), \tag{10}$$

with corresponding boundary conditions:

$$u = u_w(x) = ax, \ v = 0, \frac{\partial T}{\partial y} = -h_s T \ at \ y = 0,$$

$$u \to 0, T \to T_\infty, \ as \ y \to \infty, \tag{11}$$

where, (u, v) and (u_p, v_p) are velocity components of the fluid and dust phase of Casson fluid along the x and y axes of respectively, ρ and ρ_p are densities of fluid and dust phase of the Casson fluid respectively, T and T_p are the temperature of fluid and dust phase of the Casson fluid respectively, c_p and c_s are the specific heat capacity of fluid and dust phase of the Casson fluid, $g, \beta^*, \mu_B, \alpha, \kappa, \gamma_t, \sigma$ and $\tau_v = 1/\kappa$ are the acceleration due to gravity, thermal expansion, plastic dynamic viscosity for non-Newtonian fluid, aligned angle of magnetic field, Stokes's resistance (Drag force), thermal relaxation time, fluid electric conductivity and relaxation time of dust phase respectively. Furthermore, B_0 represents the magnetic field strength, h_S is the heat transfer parameter for Newtonian heating, a is a positive constant, and Casson parameter is given by $\beta = \mu_B \sqrt{2}$. It is worth noting that in the governing equations for two-phase Casson fluid, the governing equation for each constituted phase is formulated separately, and then coupled together via interaction terms.

For numerical purposes, governing equations (1) to (6) and (8) to (10) with corresponding boundary conditions (7) and (11) respectively are transformed into dimensionless ordinary differential equation using the following similarity variables [7,9]:

$$u = axf'(\eta), \; v = -\sqrt{a\upsilon}\,f(\eta), \; \theta(\eta) = \frac{T - T_\infty}{T_\infty}, \; \eta = \sqrt{\frac{a}{\upsilon}}\,y,$$

$$u_p = axF'(\eta), \; v_p = -\sqrt{a\upsilon}\,F(\eta), \; \theta_p(\eta) = \frac{T_p - T_\infty}{T_\infty}.$$

(12)

Here, a prime denotes differentiation with respect to η, while u and v are defined based on a stream function ψ such that $u = \dfrac{\partial \psi}{\partial y}$ and $v = -\dfrac{\partial \psi}{\partial x}$.

Applying (12) to governing equations (9) and (10) gives the dimensionless ODE for single phase Casson fluid as:

$$\left(1 + \frac{1}{\beta}\right)f'''(\eta) + f''(\eta)f(\eta) - \left(f'(\eta)\right)^2 - M\sin^2\alpha\, f'(\eta) + \lambda\theta(\eta) = 0,$$

(13)

$$\theta''(\eta) + \Pr\theta'(\eta)f'(\eta) = 0$$

(14)

Applying the same on the corresponding boundary condition (11) yields:

$$f(0) = 0, \; f'(0) = 1, \; \theta'(0) = -b(\theta(0) + 1) \; at \; \eta = 0,$$
$$f'(\eta) \to 0, \; \theta(\eta) \to 0, \; as \; \eta \to \infty.$$

(15)

Similarly, applying (12) on (2), (3), (5), and (6) gives the dimensionless ODE for two-phase Casson fluid as:

$$\left(1 + \frac{1}{\beta}\right)f'''(\eta) + f''(\eta)f(\eta) - \left(f'(\eta)\right)^2 + \phi N(F'(\eta) - f'(\eta)) - M\sin^2\alpha\, f'(\eta) + \lambda\theta(\eta) = 0,$$

(16)

$$\theta''(\eta) + \Pr\theta'(\eta)f(\eta) + \frac{2}{3}\phi N(\theta_p(\eta) - \theta(\eta)) = 0$$

(17)

$$-F''(\eta)F(\eta) + (F'(\eta))^2 + \phi(F'(\eta) - f'(\eta)) = 0$$

(18)

$$\theta_p'(\eta)F(\eta) + \frac{2}{3}\frac{\phi}{\Pr\gamma}\left(\theta(\eta) - \theta_p(\eta)\right) = 0$$

(19)

The corresponding boundary condition (7) yields:

$$f(0) = 0, \; f'(0) = 1, \; \theta'(0) = -b(\theta(0) + 1) \; at \; \eta = 0,$$
$$f'(\eta) \to 0, \; F'(\eta) \to 0, \; F(\eta) \to f(\eta), \; \theta(\eta) \to 0, \; \theta_p(\eta) \to 0 \; as \; \eta \to \infty.$$

(20)

The involved dimensionless parameters in Eq. (13) to Eq. (20) are:

Magnetic field parameter: $M = \dfrac{\sigma B_0}{a\rho}$,

Specific heat ratio of mixture: $\gamma = \dfrac{c_s}{c_p}$,

Prandtl Number: $\Pr = \dfrac{\mu c_p}{\kappa}$,

Fluid-particle interaction parameter: $\phi = \dfrac{1}{a\tau_v}$,

Dust particle mass concentration: $N = \dfrac{\rho_p}{\rho}$,

Newtonian heating (NH) conjugate parameter: $b = -h_s \left(\dfrac{\upsilon}{a}\right)^{1/2}$,

while β and α remain as defined earlier and finally,

Mixed convection parameter: $\lambda = \dfrac{Gr_x}{\mathrm{Re}_x^2}$.

Here, the local Grashof number (Gr_x) and Reynolds number (Re_x) are defined by $Gr_x = \dfrac{g\beta^* T_\infty x^3}{\upsilon^2}$ and $\mathrm{Re}_x = \dfrac{ax^2}{\upsilon}$ respectively [15]. Furthermore, by definition, thermal expansion $\left(\beta^*\right)$ is proportional to the change in length of the sheet, this led to an assumption: $\beta^* = cx$, where 'c' is a constant of proportionality with appropriate dimensions. Hence $\lambda = \dfrac{Gr_x}{\mathrm{Re}_x^2} = \dfrac{gcT_\infty}{a}$. Similar approach was utilized by Makinde and Aziz [16].

On comparing (13) and (16), it can be observed at limiting case the two equations can be reduced to be identical at $\phi = 0$. Furthermore, taking $\lambda = 0$, $\pi = \dfrac{\pi}{2}$, and $\beta \to \infty$, the studied problem can be reduced to a problem of MHD Newtonian flow over a stretching sheet in presence of transverse magnetic field as studied by Andersson *et al.,* [17]. The resulting dimensionless ordinary differential equation with the analytical solution is respectively given as:

$$f'''(\eta) + f''(\eta)f(\eta) - \left(f'(\eta)\right)^2 - Mf'(\eta) = 0, \tag{21}$$

$$f(\eta) = \dfrac{1}{\sqrt{1+M^2}}\left(1 + e^{-\eta\sqrt{1+M^2}}\right), \tag{22}$$

from which

$$-f''(0) = \frac{1}{\sqrt{1+M^2}}. \tag{23}$$

Expression (23) will be used for numerical algorithm validation.

Now referring back to the flow configurations of this study, when applied shear stress surpasses yield stress, Casson fluid starts to flow, subsequently, the layer in contact with the sheet is dragged resulting in a frictional force in the opposite direction and also heat transfer between the sheet and the fluid occurs. To analyze these phenomena, skin friction C_f and Nusselt number Nu_x defined in (24) and (25) respectively were considered.

$$C_f = \frac{\tau_w}{\rho U_w^2(x)} \tag{24}$$

$$Nu_x = \frac{xq_w}{\kappa(T_w - T_\infty)} \tag{25}$$

According to Hayat *et al.,* [18], the wall shear stress is given by $\tau_w = \left(\mu_B + \frac{\rho_y}{\sqrt{2\pi_c}} \right) \left(\frac{\partial u}{\partial y} \right)_{y=0}$ and surface heat flux is given by $q_w = -\kappa \left(\frac{\partial T}{\partial y} \right)_{y=0}$.

Substituting the above expression into (24) and (25) yields the dimensionless local skin friction $C_f \operatorname{Re}_x^{1/2}$ and local Nusselt number $Nu_x \operatorname{Re}_x^{-1/2}$ as follows:

$$C_f \operatorname{Re}_x^{1/2} = \left(1 + \frac{1}{\beta} \right) f''(0), \tag{26}$$

$$Nu_x \operatorname{Re}_x^{-1/2} = b \left(\frac{1}{\theta(0)} + 1 \right), \tag{27}$$

Where the local Reynold's number defined as $\operatorname{Re}_x = \frac{ax^2}{\upsilon}$.

Effects of physical parameters in Eq. (13) through Eq. (20) on Eq. (26) and Eq. (27) will be examined as part of flow and heat analysis in subsequent sections.

3. Numerical Methods

To proceed with numerical solutions of the obtained dimensionless ordinary differential equations (ODE), this research employed MATLAB's bvp4c ODE solver. It is a finite difference code that takes input in form of ordinary differential equations with corresponding boundary conditions as function handles, an initial guess for the solution, and an optional parameter to customize the solver's behavior, and then uses collocation method with a C^1 piece-wise cubic polynomial to

provide numerical solution for the problem [19]. For this study, A boundary layer thickness of $\eta_\infty = 8$ was chosen with a step size of 0.02, and four values were chosen for the varying parameter under consideration and applied through the use of a for loop. As for the bvp4c command codes used in this study, they input the ODE with initial and boundary conditions to the solver via argument 'OdeBVP' and 'OdeBC', they set up options for the solver via 'bvpset', initialize the solver with an initial guess via 'OdeInt', solve the BVP, generate an array of points to evaluate the solution, and then evaluate the solution at those points using 'sol = bvp4c (@OdeBVP, @OdeBC, solinit, options)'. The resulting outputs are the plots of velocity and temperature profiles, and the values of local skin friction and local Nusselt numbers for each value of the changing parameter. The overall process is depicted in Figure 2 below.
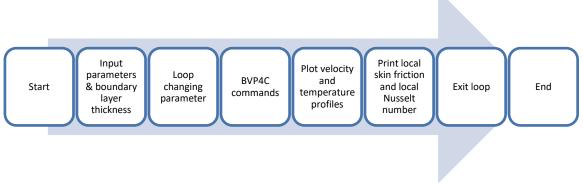

Fig. 2. BVP4C algorithm chart

4. Findings and Discussions

To ensure reliability of the of the Numerical algorithm for this study, a reliability test was done by comparing algorithm output of this study with some already established results from other studies. The values of (23) for multiple values of M as reported by Andersson *et al.,* [17] and Arifin *et al.,* [7] were considered for comparison. The output was recorded and displayed in Table 1, and as can be seen, the results are in good agreement, hence validating the numerical algorithm of the current study.
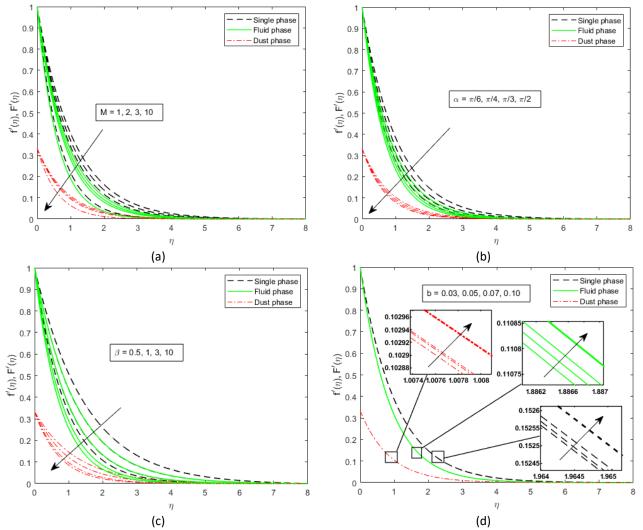
Table 1
Comparison of $f''(0)$ for different values of M when $\lambda = \phi = 0, \ \alpha = \pi/2 \ and \ \beta \to \infty$

M	Andersson *et al.,* [17] (Analytical)	Arifin *et al.,* [7] (RK45)	Present Study (BVP4C)
0.0	-1.0000	-1.0000	-1.0000
0.5	-1.2247	-1.2247	-1.2247
1.0	-1.4142	-1.4141	-1.4142
1.5	-1.5811	-1.5811	-1.5811
2.0	-1.7321	-1.7320	-1.7321

The analysis in this study is divided into two parts: flow characteristics analysis and heat transfer analysis. Flow characteristics analysis considered parameters in momentum equations i.e., Eq. (13), Eq. (16) and Eq. (18), while heat transfer analysis examined parameters in energy equation i.e., Eq. (14), Eq. (17), and Eq. (19). However, the parameters φ and N were excluded from both analyses as they are specific to two-phase Casson fluid, while parameters M and α were included in both analyses due to their direct relationship with aligned magnetic field.

Figure 3(a) to (d) illustrate the impact of parameters M, α, β, and λ on the velocity profile of single-phase and dusty Casson fluid. Table 2 presents the distribution of local skin friction for the same fluids. It can be observed that M and α decreased velocity profile and decreased local skin friction for all fluid phases. While β decreased velocity profile and increased local skin friction for all fluid phases Effects of M and α can be attributed to Lorentz forces while effect of β can be attributed to plastic dynamic viscosity.

Observing Figure 3(d) and Table 2, it is evident that an increase in λ had a negligible impact on flow properties of both fluids. Nonetheless, it increased velocity for both fluids and increased skin friction in single phase while having a relatively negligible impact on two-phase skin friction. These findings suggest that the effect of aligned magnetic field (M and α) and viscous forces (β) is more pronounced in flow properties of both fluid than buoyancy and inertia forces (λ). Furthermore, as depicted in Figure 3(a) to (d), it is evident that the velocity magnitude follows a descending order, with the single-phase Casson fluid exhibiting the highest velocity, followed by the fluid phase and the dust phase of the two-phase Casson fluid. This observation indicates that the inclusion of dust particles diminishes the flow velocity of Casson fluids within the investigated configurations.

Fig. 3. Effect of magnetic field parameter (M), aligned angle (α), Casson parameter (β), and mixed convection parameter (λ) on the velocity profile of single-phase and dusty Casson fluid Caption

Table 2
Distribution of local skin friction for single-phase and dusty Casson fluid with multiple values of M, α, β, and λ

Parameters		Single-phase Casson Fluid	Two-phase Casson Fluid
M	1	-1.3668	-1.6932
	2	-1.4974	-1.8003
	3	-1.6175	-1.9015
	10	-2.2886	-2.4975
α	$\pi/6$	-1.4335	1.7476
	$\pi/4$	-1.6175	-1.9015
	$\pi/3$	-1.7827	-2.0439
	$\pi/2$	-1.9338	-2.1770
β	0.5	-2.0292	-2.4728
	1	-1.6558	-2.0183
	3	-1.3514	-1.6475
	10	-1.2272	-1.4962
λ	0.5	-1.4347	-2.3916
	0.6	-1.4344	-2.3916
	0.7	-1.4341	-2.3916
	1.0	-1.4333	-2.3916

Table 3 presents the impact of parameters M, α, b, and Pr on distribution of local Nusselt number for single-phase and dusty Casson fluid, while Figure 4(a) to Figure 4(d) displays the impact the same parameters on their temperature profiles. On observing these, it can be noted that the temperature profile and consequently thermal boundary layer thickness increased for all flow phases due to an increase in M, α, and b, while they decreased with increase in Pr. Additionally, Nusselt number decreased with M and α and increased with b and Pr.
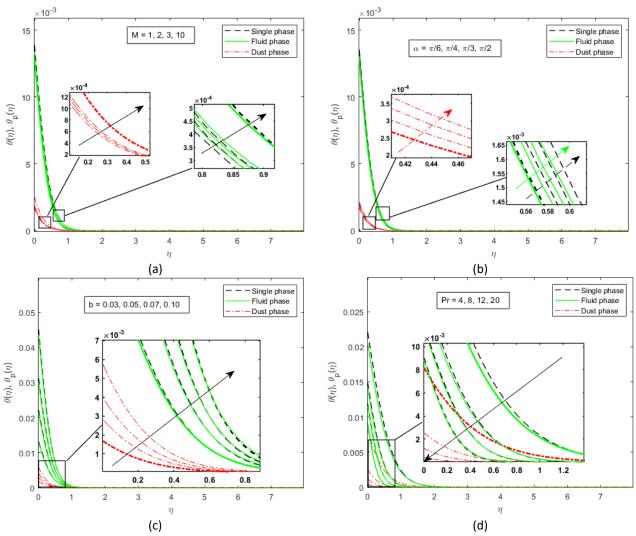
Table 3
Distribution of local Nusselt number for single-phase and dusty Casson fluid with multiple values of M, α, b, and Pr

Parameters		Single-Phase Casson Fluid	Two-Phase Casson Fluid
M	1	2.3272	2.3994
	2	2.3083	2.3842
	3	2.2908	2.3700
	10	2.1930	2.2857
α	$\pi/6$	2.3175	2.3917
	$\pi/4$	2.2908	2.3700
	$\pi/3$	2.2668	2.3498
	$\pi/2$	2.2448	2.3310
b	0.03	2.3175	2.3917
	0.05	2.3177	2.3918
	0.07	2.3179	2.3920
	0.10	2.3182	2.3922
Pr	4	1.3894	1.4959
	8	2.5509	2.1355
	12	2.5585	2.6240
	10	3.3632	3.4055

Fig. 4. Effect of magnetic field parameter (M), aligned angle (α), NH conjugate parameter (b) and Prandtl number (Pr) on the velocity profile of single-phase and dusty Casson fluid

Effects of M and α on temperature profile, thermal boundary layer and local Nusselt number suggests that a stronger aligned magnetic field leads to a relatively high temperature variations in the boundary layer while decreasing convective heat transfer properties of both fluids. This effect can be attributed to Joule heating effects which is essentially the heating caused by the interaction between magnetic fields and electrically conducting fluids [20].

The effect of b can be explained by the relationship between b, heat transfer coefficient (h_s) and kinematic viscosity υ, where $b = -h_s\sqrt{a/\upsilon}$. An increase in b leads to a higher heat transfer or lower viscosity, both of which contribute to increased temperature variations across the boundary layer and consequently a more efficient heat transfer rate.

Regarding Pr, it has been established that increasing Pr signifies a slower heat (thermal) diffusion which implies a thinner thermal boundary layer and consequently less temperature gradient [13]. This explains the observed decline in temperature profile and thermal boundary layer. Additionally, a smaller thermal diffusion implies a weaker heat conduction consequently allowing heat convection to dominate the heat transfer mechanism, hence the increase in Nusselt number.

Furthermore, it can be observed from the distribution of temperature profiles in Figure 4(a) through Figure 4(d) that the impact of the parameters b and Pr on temperature profiles is more pronounced compared to the parameters M and α. This implies that under the considered

configuration, thermal and momentum diffusivity, along with the NH conditions, play a more significant role in influencing temperature changes than the influence of an aligned magnetic field. Moreover, as depicted in Figure 4 (a) to Figure 4(d), similar to velocity profile, the temperature magnitude follows a descending order, with the single-phase Casson fluid exhibiting the highest magnitude, followed by the fluid phase and the dust phase of the two-phase Casson fluid. This observation indicates that the inclusion of dust particles diminishes the temperature variations of Casson fluids within the investigated configurations.

5. Conclusion

Based on the conducted comparative analysis of the findings for single-phase and two-phase Casson fluid, the following conclusions can be drawn:
  i.   Both fluids exhibited similar changes in flow and thermal properties when the studied parameters were modified, hinting a consistent relationship between the two fluids.
 ii.   A stronger aligned magnetic field implies a slower flow with less friction leading to higher temperature variations with less convective heat transfer in both fluids.
iii.   NH conditions enhance temperature variations and improved convective heat transfer in both fluids.
 iv.   The influence of an aligned magnetic field and viscous forces dominates over buoyancy and inertia forces in determining the flow characteristics of both fluids.
  v.   The NH condition, momentum and thermal diffusivity have a stronger impact on the thermal characteristics of both fluids compared to the aligned magnetic field.
 vi.   The analysis of velocity and temperature magnitudes revealed that the single-phase consistently exhibited higher values regardless of the parameter variations followed by the fluid-phase of the dusty Casson fluid and then the dust-phase with the lowest magnitudes. These findings suggest that the presence of dust particles reduces the velocity and temperature magnitudes of the Casson fluid. Similar conclusions have also been reported in previous studies by Arifin *et al.,* [7] and Kasim *et al.,* [9] when investigating the interaction between the fluid-phase and dust-phase of the two-phase Casson fluid using the fluid-particle interaction parameter (ϕ).

To finalize, the authors recommend further investigations to consider other fluids types such as nanofluids and ferrofluids, different flow conditions such as slip flow or convective boundary conditions, and other complex geometries such as cylindrical or spherical bodies for more insights in to the intricacies of single and two-phase flow.

References
[1]   Merkin, J. H. "Natural-convection boundary-layer flow on a vertical surface with Newtonian heating." *International Journal of Heat and Fluid Flow* 15, no. 5 (1994): 392-398. https://doi.org/10.1016/0142-727X(94)90053-1
[2]   Lesnic, D., D. B. Ingham, and I. Pop. "Free convection boundary-layer flow along a vertical surface in a porous medium with Newtonian heating." *International Journal of Heat and Mass Transfer* 42, no. 14 (1999): 2621-2627. https://doi.org/10.1016/S0017-9310(98)00251-8
[3]   Lesnic, Daniel, Derek B. Ingham, and Ioan Pop. "Free convection from a horizontal surface in a porous medium with Newtonian heating." *Journal of Porous Media* 3, no. 3 (2000). https://doi.org/10.1615/JPorMedia.v3.i3.40

[4]   Lesnic, D., D. B. Ingham, I. Pop, and C. Storr. "Free convection boundary-layer flow above a nearly horizontal surface in a porous medium with Newtonian heating." *Heat and Mass Transfer* 40 (2004): 665-672. https://doi.org/10.1007/s00231-003-0435-y

[5]   Reyaz, Ridhwan, Ahmad Qushairi Mohamad, Yeou Jiann Lim, and Sharidan Shafie. "Analytical Solutions for Fractional Caputo-Fabrizio Casson Nanofluid on Riga Plate with Newtonian Heating." *Journal of Advanced Research in Applied Sciences and Engineering Technology* 29, no. 1 (2022): 142-159. https://doi.org/10.37934/araset.29.1.142159

[6]   Mohamed, Muhammad Khairul Anuar, Siti Hanani Mat Yasin, Mohd Zuki Salleh, and Hamzeh Taha Alkasasbeh. "MHD stagnation point flow and heat transfer over a stretching sheet in a blood-based casson ferrofluid with newtonian heating." *Journal of Advanced Research in Fluid Mechanics and Thermal Sciences* 82, no. 1 (2021): 1-11. https://doi.org/10.37934/arfmts.82.1.111

[7]   Arifin, Nur Syamilah, Syazwani Mohd Zokri, Abdul Rahman Mohd Kasim, Mohd Zuki Salleh, Wan Nur Syahidah Wan Yusoff, Nurul Farahain Mohammad, and Sharidan Shafie. "Aligned magnetic field on dusty Casson fluid over a stretching sheet with Newtonian heating." *Malaysian Journal of Fundamental and Applied Sciences* 13, no. 3 (2017): 245-248. https://doi.org/10.11113/mjfas.v13n3.592

[8]   Arifin, Nur Syamilah, Abdul Rahman Mohd Kasim, Syazwani Mohd Zokri, Siti Farah Haryatie, and Mohd Zuki Salleh. "Dusty Casson Fluid Flow containing Single-Wall Carbon Nanotubes with Aligned Magnetic Field Effect over a Stretching Sheet." *CFD Letters* 15, no. 1 (2023): 17-25. https://doi.org/10.37934/cfdl.15.1.1725

[9]   Kasim, Abdul Rahman Mohd, Nur Syamilah Arifin, Syazwani Mohd Zokri, Mohd Zuki Salleh, Nurul Farahain Mohammad, Dennis Ling Chuan Ching, Sharidan Shafie, and Noor Amalina Nisa Ariffin. "Convective transport of fluid-solid interaction: A study between non-Newtonian Casson model with dust particles." *Crystals* 10, no. 9 (2020): 814. https://doi.org/10.3390/cryst10090814

[10]   Arifin, Nur Syamilah, Abdul Rahman Mohd Kasim, Syazwani Mohd Zokri, and Mohd Zuki Salleh. "Boundary Layer Flow of Dusty Williamson Fluid with Variable Viscosity Effect Over a Stretching Sheet." *Journal of Advanced Research in Fluid Mechanics and Thermal Sciences* 86, no. 1 (2021): 164-175. https://doi.org/10.37934/arfmts.86.1.164175

[11]   Eldabe, Nabil Tawfik, Mohamed Yahya Abouzeid, and Hemat A. Ali. "Effect of heat and mass transfer on Casson fluid flow between two co-axial tubes with peristalsis." *Journal of Advanced Research in Fluid Mechanics and Thermal Sciences* 76, no. 1 (2020): 54-75. https://doi.org/arfmts.76.1.5475

[12]   Azmi, Wan Faezah Wan, Ahmad Qushairi Mohamad, Lim Yeou Jiann, and Sharidan Shafie. "Analytical Solution of Unsteady Casson Fluid Flow Through a Vertical Cylinder with Slip Velocity Effect." *Journal of Advanced Research in Fluid Mechanics and Thermal Sciences* 87, no. 1 (2021): 68-75. https://doi.org/10.37934/arfmts.87.1.6875

[13]   Mukhopadhyay, Swati. "Casson fluid flow and heat transfer over a nonlinearly stretching surface." *Chinese Physics B* 22, no. 7 (2013): 074701. https://doi.org/10.1088/1674-1056/22/7/074701

[14]   Mukhopadhyay, Swati, Krishnendu Bhattacharyya, and Tasawar Hayat. "Exact solutions for the flow of Casson fluid over a stretching surface with transpiration and heat transfer effects." *Chinese Physics B* 22, no. 11 (2013): 114701. https://doi.org/10.1088/1674-1056/22/11/114701

[15]   Mohamed, M. K. A., M. Z. Salleh, N. A. Z. Noar, and A. Ishak. "Buoyancy effect on stagnation point flow past a stretching vertical surface with Newtonian heating." In *AIP Conference Proceedings*, vol. 1795, no. 1. AIP Publishing, 2017. https://doi.org/10.1063/1.4972149

[16]   Makinde, Oluwole D., and A. Aziz. "Boundary layer flow of a nanofluid past a stretching sheet with a convective boundary condition." *International Journal of Thermal Sciences* 50, no. 7 (2011): 1326-1332. https://doi.org/10.1016/j.ijthermalsci.2011.02.019

[17]   Andersson, H. I., K. H. Bech, and B. S. Dandapat. "Magnetohydrodynamic flow of a power-law fluid over a stretching sheet." *International Journal of Non-Linear Mechanics* 27, no. 6 (1992): 929-936. https://doi.org/10.1016/0020-7462(92)90045-9

[18]   Hayat, T., M. Awais, S. Asghar, and Awatif A. Hendi. "Analytic solution for the magnetohydrodynamic rotating flow of Jeffrey fluid in a channel." *Journal of Fluids Engineering* 133, no. 6 (2011): 061201. https://doi.org/10.1115/1.4004300

[19]   Kierzenka, Jacek, and Lawrence F. Shampine. "A BVP solver based on residual control and the Maltab PSE." *ACM Transactions on Mathematical Software (TOMS)* 27, no. 3 (2001): 299-316. https://doi.org/10.1145/502800.502801

[20]   Swain, B. K., B. C. Parida, S. Kar, and N. Senapati. "Viscous dissipation and joule heating effect on MHD flow and heat transfer past a stretching sheet embedded in a porous medium." *Heliyon* 6, no. 10 (2020). https://doi.org/10.1016/j.heliyon.2020.e05338